Active submillimeter diagnostics of the plasma of a microwave pinch discharge at high pressure

É. A. Tishchenko and V. G. Zatsepin

Physics Laboratory, USSR Academy of Sciences
(Submitted August 2, 1974)
Zh. Eksp. Teor. Fiz. **68**, 547–561 (February 1975)

The technical and methodological aspects of active submillimeter diagnostics of the plasma of a pinch discharge rotating along irregular trajectories about the axis of a microwave cavity under the action of a stabilizing gas flow are described. The rotation is used for transverse probing of the pinch by converging microwave beams which are narrow enough compared with the characteristic pinch diameter. The cutoff method for determining the maximum electron density at the axis of a radially inhomogeneous plasma cylinder under conditions of strong refraction is substantiated and generalized in the quasioptical approximation. The accuracy of the results obtained by the cutoff method (estimated to be $\sim 10\%$) is confirmed by observations of signals reflected from the plasma. A method is developed for measuring the characteristic pinch diameters at a level of 10% of the maximum concentration. Simultaneous four-frequency transverse probing is used to determine the electron-density distribution function averaged over the probing-beam width. The maximum electron density (10^{15}–10^{16} cm^{-3}) and characteristic diameter (2–10 mm) of a discharge in deuterium are measured in a small plasma installation at a gas pressure 1–2 atm. and at a microwave input power 4–12 kW. In a plasma installation that is three time larger, these parameters are respectively 10^{15}–10^{17} cm^{-3} and 4–25 mm at pressures between 1 and 5 atm. and at an input power between 15 and 40 kW. At equal pressures and electron density the diameters of the large-installation plasma pinch is almost three times that in the small installation. The pinch diameter decreases with increasing pressure at a fixed power. Time-dependent fluctuations of the plasma-pinch structure and of the electron-density profile are observed, with an abrupt jump of the plasma density near the axis.

1. INTRODUCTION

P. L. Kapitza [1-3] has described methods of obtaining microwave discharge pinches in deuterium gas at high pressure, as well as experimental and theoretical investigations of these discharges and the prospects for their utilization. Spectrometric and current investigations, and also their theoretical interpretation, have led to the conclusion that the discharge consists of an internal cylindrical region (core) filled with hot plasma with an electron temperature on the order of 10^6 °K, and a surrounding cloud (jacket) of partially ionized plasma with temperature less than 10^4 °K. It is assumed that the elastic reflection of the electrons from the double layer that exists on the boundary of these two regions ensures thermal insulation of the hot electronic components of the plasma. Optical measurements described in [1] gave information on the outer part of the discharge, but although passive diagnostics in the far infrared region of the spectrum did yield (on the basis of the radiation cutoff) data on the electronic component of the core, these data could not be resolved in time or space because of the low signal/noise ratio.

The development of backward-wave tubes [4] and of lasers operating in the submillimeter band (0.1–1 mm), which contains the characteristic plasma frequencies of the investigated discharge, has made it possible to carry out active diagnostics by passing converging microwave beams through the pinch. The natural irregular rotation of the discharge around the resonator axis, with frequency 5–20 Hz, was used to effect transverse (along the chords) probing with beams that were narrow enough in comparison with the characteristic dimension of the plasma.

The encountered technical difficulties were connected mainly with the insufficient commercial development of the submillimeter band. Quasioptical waveguide elements and helium cryostats were developed and constructed for the radiation detectors. The diagnostics of a pinch discharge at high pressure (3–5 atm) became possible through the use of a submillimeter laser operating on ordinary and heavy water vapor and generating a number of lines in the range 40–220 μ. This laser was developed by G. D. Bogomolov and V. V. Zav'yalov and constructed in the machine shop of the Institute.

Rotation of the pinch with velocity 0.1–1 m/sec made it necessary to replace the inertial carbon bolometers used in passive diagnostics by high-speed detectors, cooled to 4°K, based on n-InSb in the long-wave part ($\lambda \gtrsim 200\ \mu$) and based on GeB in the short-wave part of the investigated band. Information on the experimental setup are given in Sec. 2.

Certain difficulties of methodological character were also overcome. The cutoff method used in microwave diagnostics in the geometrical-optics approximation for a plane layer was modified and applied to a radially inhomogeneous plasma cylinder in the case of strong refraction, when the plasma dimension did not greatly exceed the dimension of the sounding beam. By model experiments with metallic cylinders and cavities in paraffin blocks that imitated the transcritical and subcritical plasma, supplemented with calculations of the refraction for an inhomogeneous plasma, it was verified that the cutoff method is applicable and an estimate of its accuracy under real experimental conditions was obtained. In addition, a method was developed for measuring the characteristic diameters of the discharge at a level of 10% of the maximum concentration (see Secs. 3 and 4).

Active diagnostics was used to obtain more precise data on the electronic structure of the pinch discharge with a smaller experimental setup. The presence of time fluctuations of the pinch structure has made it necessary to carry out simultaneous four-frequency probing (see Secs. 2, 4, and 5) to obtain, with one passage of the pinch

through the probing beams, information not only on its maximum concentration but also on the concentration profile, using the procedure described in Sec. 3. The results of the measurement of the radiation scattered by the plasma are described and confirm the concentration data obtained by the cutoff method (Sec. 5).

A pinch discharge was investigated in an installation three times larger than the one described in [1]. Data on its construction will be published later. The increase of the transverse dimensions of the pinch by almost three times, and the decrease of the wavelength of the probing radiation for the increased-pressure regimes, have permitted a more detailed study of the discharge structure. Besides the monotonically decreasing concentration profiles, profiles were observed with an abrupt density discontinuity in the region next to the axis.

The work described here was carried out at the Physics Laboratory of the USSR Academy of Sciences under the leadership of Academician P. L. Kapitza for four years. N. V. Filimonova took part in the construction of the quasioptical waveguide elements, and K. A. Zhdanov participated in the development of the electronic instruments. The experiments were performed with the help of S. I. Filimonov, N. I. Kondrat'ev, A. V. Lebedev, V. I. Chekin, V. B. Lazarev, and A. N. Demin. G. P. Prudkovskiĭ and B. P. Belov helped with the calculations of the refraction with the trajectory-plotting analog computer.

2. EXPERIMENTAL SETUP

The measurement setup normally employed in the experiment is shown in Fig. 1. The microwave power is radiated from the open end of a multiwave waveguide of a backward-wave tube (BWT). This end is located at the focus of a teflon lens 1 of 50 mm diameter and focal length 150 mm, which transforms the radiation into a parallel beam. After passing through a system of two one-dimensional polarizing grids 2 and 4 and a three-mirror polarization rotator 3, the beam is incident on a lens-window 5 of a microwave resonator. The lens focuses the beam on the axis of the resonator, in the region where the plasma pinch 6 rotates. The radiation emerges through an identical lens-window 7 and is registered with an InSb detector placed in a helium cryostat at 4.2°K. The radiation scattered by the plasma pinch upward at an angle 90° to the beam axis is gathered by a teflon lens 8 and is registered by a similar InSb receiver.

Quartz lenses 9 and 10 and two pairs of photocells 11 and 12 constitute the optical part of the system for registering the discharge coordinates.

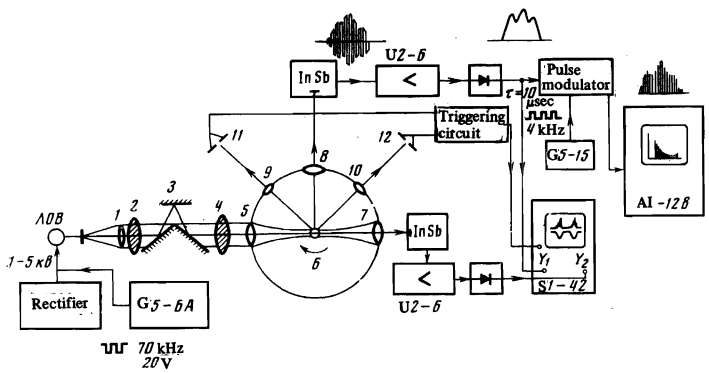

FIG. 1. Block diagram of measurement setup (the notation is explained in the text.

Lenses 1, 5, 7, and 8 are prepared of ftoroplast-4 teflon, the dielectric constant of which does not depend on the frequency in the investigated wavelength range and is equal to $\epsilon_0 = 2.05$, i.e., the refractive index is $n = 1.43$. The lenses are made planoconvex. Their convex surface is spherical in shape. They were produced on a lathe and then polished with drawing paper. In the small plasma installation, lenses 5 and 7 had a diameter 27 mm and a focal length 150 mm, while in the larger installation the respective values were 50 and 360 mm. A study of the distribution of the microwave-beam power in the focus of the lenses has shown that the beam is close enough to Gaussian with a half-width on the order of (6—8) λ.

The teflon lenses served simultaneously as the vacuum-tight windows of the microwave resonator. They could withstand a differential pressure up to 4 atm without noticeable change in their optical characteristics. The vacuum seal was provided by rubber and indium gaskets, and the mechanical stability of the windows was ensured by the presence on the lens periphery of projections that fitted in slots of the lens frames.

To filter out the higher modes and to ensure purity of the polarization of the radiation incident on the plasma, we used one-dimensional wire grids 2 and 4. The grids had a period of 60 μ and were stretched on rings of 80 mm diameter.

The three-mirror polarization rotator 3 made it possible to rotate the polarization direction of the microwave radiation without shifting the beam axis and without changing the spatial distribution of the power. This ensured the possibility of exactly measuring the polarization effects produced by interaction between the radiation and the plasma. In experiments with different polarizations, the direction of the electric-field vector of the wave was set with the aid of the rotator 3 at an angle 45° to the pinch axis. By rotating the polarizer 4 it was possible to separate two polarizations of equal intensity and with the required field direction, along the pinch axis and perpendicular to it, without upsetting the shape of the beam or its position in space.

Lavsan polyester films and two-dimensional metallic grids were used as the power beam splitters. To absorb parasitic radiation (scattered by the frames of the optical elements and the surrounding objects), sponge rubber was used, as well as "porolon" impregnated with a suspension of aquadag in an acqueous solution of the BF-6 adhesive.

The optical channel of the radiation receiver placed in a helium Dewar is described in detail in [5]. The aperture angle of the directivity pattern of the receiving unit is 7° at the 3-dB level. The diameter of the entrance window of the cryostat is 8 mm. To improve the spatial resolution, the detector is located ~0.8 m away from the entrance lens for the smaller installation and ~2 m for the larger installation.

Figure 1 shows only one channel for the measurement of the plasma transmission coefficient. It has become possible by now to measure simultaneously the transmission signal at four different frequencies. In this scheme one uses two backward-wave tubes, the radiation from which, modulated at different frequencies (40 and 70 kHz), is directed along the optical axis of the system

and is registered by one InSb detector. The signal from the detector is divided into two channels with the aid of narrow-band tuned amplifiers. On the other side of the microwave resonator, along the same optical axis, is directed the radiation of a submillimeter laser, which generates simultaneously at two wavelengths, 0.118 and 0.22 mm. These radiations are modulated in amplitude at frequencies 35 and 15 kHz, respectively. The radiation at λ = 0.22 mm is registered with an In-Sb detector, and the signal at λ = 0.118 mm is received with a GeB detector.

The series of broadband traveling-wave tubes covers the spectrum from 0.3 to 2 mm. The tubes can be smoothly tuned electronically in a range on the order of an octave. The radiation power of these tubes reaches several dozen milliwatts. The long-time stability of the microwave power during the course of the experiment was maintained within 1—3%.

For microwave diagnostics of a discharge at the increased pressure, at which electron density was increased to 10^{17} cm^{-3}, we used the radiation of a submillimeter laser. At a discharge-space length ~ 3 m and a mirror diameter 80 mm (one spherical and the other flat in the form of a two-dimensional grid with mesh 30 μ), the laser radiation power was several dozen milliwatts. The submillimeter lasing was in the cw mode on lines of H_2O (0.079, 0.118, and 0.22 mm) and of D_2 (0.172 mm), and also of HCN (0.337 mm). The laser radiation was modulated in amplitude at a frequency 15—50 kHz as the result of beats between two oscillation modes.

The radiation was registered with bolometers cooled to helium temperatures and with photoconductivity-receivers. A carbon bolometer with operating time $\tau \approx 1$ msec at 2° K worked in the entire investigated frequency range; the receiver based on InSb, with $\tau \lesssim 1$ μsec at 4° K registered the radiation with $\lambda \gtrsim 0.2$ mm. To receive radiation at the laser lines with $\lambda \leq 0.118$ mm, we used an impurity photoconductivity GeB detector.

To improve the signal/noise ratio of the recording system we used resonant amplification of signals from detectors at the carrier frequency of the microwave-generator modulation. The signal modulation was useful also because it eliminated the null drift of the dc amplifiers. To increase the operating speed of the apparatus, the modulation frequency of the backward wave tubes was increased to 50—70 kHz. Since the tube generation bands are highly chopped up, variation of the BWT collector voltage by 5—20 V can yield amplitude modulation of the radiation, with depth 30—60%, in the entire tuning range. The radiation frequency changes by not more than 0.1% at this value of the modulation. The modulation was obtained by adding to the high-voltage supply voltage a small pulsed component from a G5-6A generator (Fig. 1).

The alternating signals from the detectors were amplified with tuned amplifiers U2-6 (bandwidth equal to 10% of the carrier frequency), were detected, and were smoothed out with a time constant 300 μsec. The envelopes of the rectified microwave transmission and reflection signals were fed to the input of long-persistence oscilloscopes S1-42 and S1-29. The oscilloscopes operated in the slaved regime and were triggered by a special system that registered the coordinates of the plasma pinch at the instant when the plasma axis passed through a previously chosen "aiming point."

In the multiple-frequency probing of the plasma, all four transmission signals were observed simultaneously on the screen of one oscilloscope using standard switching attachments from the S1-15 oscilloscope. Signals from two channels were fed to an electronic switch that alternately switched them at 50 kHz, applying them simultaneously with a relative bias to the input of the amplifier of the first beam of the S1-42 oscilloscope. Similarly, the two other channels were registered by the second split beam of the oscilloscope.

In view of the unsatisfactory reproducibility and low intensity of the reflection signals, they were studied by averaging with the aid of multichannel pulse-height analyzers. To this end, a system was developed for the measurement of the extremal values and for the integration of rapidly varying irregular signals [6].

The transverse multichord probing was made possible under our conditions by the fact that, owing to its rotation, the plasma pinch crossed the microwave beam in the focal plane of lenses 5 and 7 (see Fig. 1). The transmission signal T was registered as a function of the impact parameter ρ, namely the distance between the axis of the pinch and of the probing beam. To measure the impact parameter ρ, we developed a system of registering the coordinates of the discharge axis [7]. This system triggered measuring apparatus at instants of time when the discharge axis passed through a previously chosen aiming point in the focal plane of the lenses at a distance ρ from the beam axis, with accuracy $\Delta\rho$ = 0.2—0.3 mm.

3. REFRACTION OF RAYS IN A RADIALLY INHOMOGENEOUS PLASMA CYLINDER

For a quantitative interpretation of the experimental transmission curves $T(\rho)$, we consider in the homotropic approximation the refraction of beams that enter in a radially inhomogeneous plasma cylinder at an impact distance ρ (see Fig. 2) from its axis. Let the dielectric constant of the plasma be

$$\varepsilon(r)=1-\gamma n_e(r)/n_e(0), \tag{1}$$

where $\gamma = \omega_0^2/\omega^2$; $\omega_0^2 = 4\pi n_e(0)e^2/m$ is the plasma frequency on the cylinder axis, ω is the frequency of the sounding radiation; $n_e(r)/n_e(0)$ is the electron density distribution function. The case $\gamma < 1$ will be called transcritical, and $\gamma > 1$ subcritical. By a we denote the radius of the cylinder at which $n_e(a)/n_e(0) = 0.1$, i.e., $\epsilon(r) \approx 1$ at $r \gtrsim a$.

From the refraction law we can obtain a differential equation for the beam trajectory [8] in a polar coordinate system (r, φ) connected with the cylinder axis

$$d\varphi/dr=\rho/r\sqrt{\varepsilon r^2-\rho^2}. \tag{2}$$

It is seen from Fig. 2 that the beam passing through the plasma is deflected from the initial direction by an angle θ equal to

$$\theta=\pi-2\varphi_0-2\varphi=\pi-2\arcsin\frac{\rho}{a}-2\int_{r_c}^{a}\frac{\rho\,dr}{r\sqrt{\varepsilon r^2-\rho^2}}, \tag{3}$$

where r_c is the root of the equation $\epsilon(r_c)r_c^2 = \rho^2$.

We consider refraction in the simplest case, by a plasma cylinder with homogeneous concentration distribution. This example will demonstrate all the character-

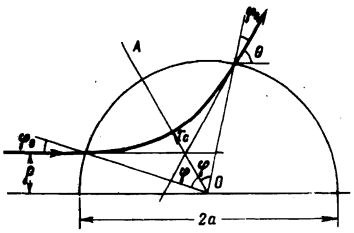

FIG. 2

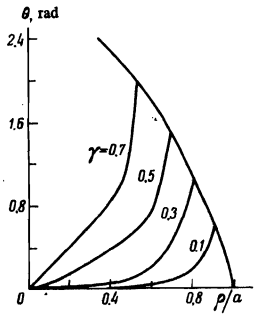

FIG. 3

FIG. 2. Refraction in an inhomogeneous plasma cylinder.

FIG. 3. Refraction angle of a beam in a homogeneous plasma cylinder.

istic features of refraction by a cylinder, features used in the calibration of the optical system of the installation.

From (3) we obtain for the refraction angle θ the expression

$$\theta=2\left(\arcsin\frac{\rho}{a\sqrt{1-\gamma}}-\arcsin\frac{\rho}{a}\right). \qquad (4)$$

For impact parameters $\rho > \rho_1 = a\sqrt{1-\gamma}$, the beam does not enter the cylinder and experiences total internal reflection on the surface. At $\rho = \rho_1$, the deflection angle is maximal and equal to $\theta_1 = 2\sin^{-1}\sqrt{\gamma}$. Figure 3 shows a family of curves $\theta(\rho/a)$ for a homogeneous profile at different values of γ. It is seen from the plots that for a subcritical plasma ($\gamma < 1$) there exists two impact parameters $\rho = \pm\rho_1$, at which the beam experiences maximum deflection and the transmission signal experiences maximum attenuation because of the finite angular aperture of the receiving system. When the plasma pinch passes through a probing beam, this is expressed in the appearance of two minima in the transmission curve $T(\rho)$ (see Fig. 9 below). For a transcritical homogeneous plasma ($\gamma > 1$), the beam is reflected as if from a metallic cylinder. The angular distribution of the reflected radiation is then given by

$$\theta=2\arcsin\sqrt{1-(\rho/a)^2}. \qquad (5)$$

When the transcritical cylinder passes through the microwave beam, the transmission signal $T(\rho)$ contains only one minimum at $\rho = 0$, as follows from (5). Calibration $T(\rho)$ curves for metallic cylinders were used to eliminate the finite width of the sounding beam when the characteristic dimensions of the discharge were determined.

It is clear from the foregoing that on going through the critical frequency ($\gamma = 1$) a change will take place in the form of the transmission curve $T(\rho)$. This was used to determine the maximum electron density on the axis of the plasma cylinder. The method is a generalization of the cutoff method used in microwave diagnostics to the case of a radially inhomogeneous plasma under strong refraction conditions.

To study the influence of the shape of the profile of the electron concentration on the results of the measurements of the transmission signals, we have considered the refraction of the probing beams by several types of greatly differing profiles—see Fig. 4, namely uniform (curve 1), and exponential specified by the formula

$$\frac{n_e(r/a)}{n_e(0)}=\exp\left[\left(\frac{r}{a}\right)^{\alpha}\ln 0.1\right], \qquad (6)$$

where $\alpha = 6$ (curve 2), $\alpha = 4.5$ (curve 3), $\alpha = 2$ (curve 4), and $\alpha = 1$ (curve 5). By a we denote the plasma radius at which $n_e(a) = 0.1n_e(0)$.

FIG. 4. Calculated concentration profiles (the marking of the curves is explained in the text).

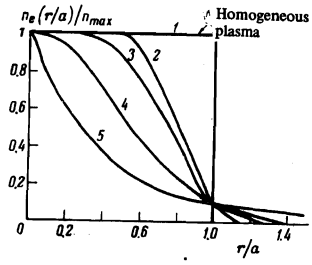

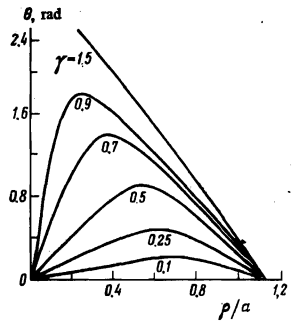

FIG. 5

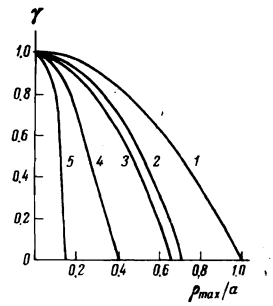

FIG. 6

FIG. 5. Refraction angles for the profile 2 of Fig. 4.

FIG. 6. Theoretical dependence of $\gamma = n_0/n_c$ on ρ_{max}/a. The number of the curves correspond to Fig. 4.

The calculation of the deflection angles $\theta(\rho)$ of the beams incident on the plasma cylinder with different impact parameters ρ was carried out by numerically integrating Eq. (3) and using (1).

By way of example we consider the results of a calculation of the refraction angle θ at different γ for the profile corresponding to curve 2 of Fig. 4. As seen from the plots of Fig. 5, just as for the homogeneous case, there is a characteristic maximum of the deflection angle at $\rho = \pm\rho_1$ for a subcritical plasma ($\gamma < 1$). At $\gamma > 1$, the central part of the pinch is opaque to the radiation and the angle θ increases monotonically as ρ decreases to zero. Thus, for an inhomogeneous plasma, a change in the shape of the transmission signal will likewise take place on passing through the critical concentration ($\gamma = 1$).

From the family of $\theta(\rho/a)$ curves we obtain for each of the concentration profiles represented in Fig. 4 the dependence of the impact parameter ρ_{max}/a corresponding to the maximum angle of deflection, on the value of γ, i.e., on the frequency of the sounding radiation. This has made it possible to determine the shape of the concentration profile by measuring in experiment the connection between γ and ρ_{max}/a and then comparing it with the theoretical relations shown for the calculated profiles in Fig. 6. The value of ρ_{max} is determined from the experimental transmission curves $T(\rho)$, which have at $\rho = \pm\rho_{max}$ two characteristic minima in the subcritical case.

With the aid of a trajectory-plotting analog computer [9] we investigated also certain special concentration profiles, namely nonmonotonic, with a dip in the region near the axis, and profiles with a concentration jump at the axis. Such profiles are quite easy to simulate in an electrolytic bath, and the results of the calculations are obtained immediately in a lucid and easily interpreted form. The calculated concentration profiles are shown in Fig. 7a, namely a profile with a concentra-

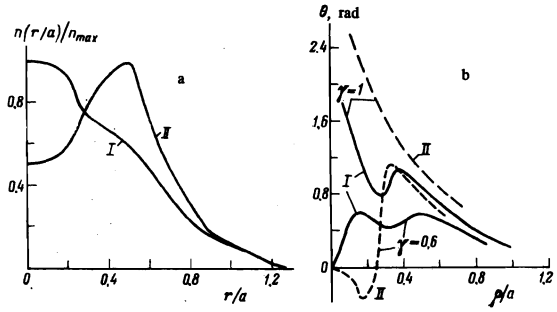

FIG. 7. a)Calculated concentration of profiles with a jump and with a dip of the concentration near the axis. b—Refraction angles for profiles I and II.

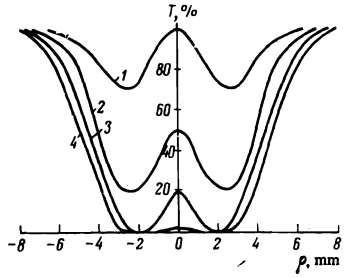

FIG. 8

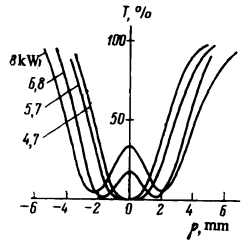

FIG. 9

FIG. 8. Transmission signals at wavelengths λ = 0.118 mm (1), 0.22 mm (2), 0.307 mm (3), and 0.43 mm (4). Deuterium, pressure P = 1.5 atm, W = 21 kW.

FIG. 9. Experimental transmission curves for various microwave power inputs. Deuterium, P = 1.3 atm, λ = 0.55 mm.

tion peak (I) and a profile with a dip in the axial region (II).

The resultant plots of $\theta(\rho/a)$ are shown in Fig. 7b for the profile with the dip (II) and for the profile with the concentration peak (I). As seen from plots I, at $\gamma < 1$ the function $\theta(\rho/a)$ has two maxima, at $\rho = \rho_1$ and $\rho = \rho_2$. The plasma with such a profile can be regarded as an aggregate of two plasma cylinders—a denser internal cylinder imbedded in a less dense external one. Each cylinder has its own impact distance ρ_1 and ρ_2 at which the maximum deflection angles of the probing beam are observed.

For $\gamma \geq 1$, the central part of the pinch becomes opaque and the local transmission maximum at $\rho = 0$ vanishes. In the transmission signal there should be observed three minima, at $\rho = 0$ and $\rho = \pm\rho_2$. With further lowering of the frequency of the probing radiation ($\gamma \gg 1$), the local maxima of the function $\theta(\rho/a)$ at $\rho = \pm\rho_2$ vanish and the signal $T(\rho)$ has a single minimum at $\rho = 0$.

For the profile with a concentration dip (curves II on Fig. 7b) the function $\theta(\rho/a)$ has in the subcritical case ($\gamma < 1$) a local minimum at $\rho = \rho_1$ and a local maximum at $\rho = \rho_2$. Therefore the transmission signal $T(\rho)$ should also have in this case four minima, at $\rho = \pm\rho_1$ and $\rho = \pm\rho_2$. For a transcritical plasma, unlike the preceding case, the central region of the discharge becomes opaque and the transmission signal is transformed immediately from a curve with four minima into a curve with one minimum at $\rho = 0$.

In the experiment, by varying the wavelength of the probing radiation, we can distinguish between the considered types of profiles and estimate the dimension of the internal region of the plasma pinch in which a sufficiently abrupt growth or decrease of the electron concentration takes place, by studying the waveform of the transmission signal. Just as in the case of the simpler profiles, this study is possible only if the width Δ of the probing beam is small ($\Delta < \rho_2 - \rho_1$). It should be noted that transmission signals corresponding to the jump of the concentration in the near-axial region of the discharge were observed in experiments on the large plasma installation (see Fig. 13 below), thus confirming the assumed model of the plasma-pinch structure.

4. PROCEDURE FOR DETERMINING THE PLASMA PARAMETERS FROM MEASUREMENTS OF THE TRANSMISSION AND REFLECTION SIGNALS

A study of the wave form of the transmission signals $T(\rho)$ yields information on the maximum concentration of the electrons and on its spatial distribution. The maximum concentration for a fixed plasma regime is determined from the frequency of the probing radiation at which a transition takes place from blocked transmission signals corresponding to the transcritical plasma ($\gamma > 1$), to unblocked signals, which have a local transmission maximum at $\rho = 0$. Thus, e.g., in Fig. 8 the wavelength $\lambda = 0.43$ mm is critical. All the remaining cases are subcritical. Usually the discharge parameters fluctuate from passage to passage through the beam, and the mean value of the maximum concentration is chosen to be the concentration $n_c = \pi mc^2/e^2\lambda^2$ corresponding to a probing wavelength λ_c such that an approximately equal number of passes with blocked and unblocked transmission signals are observed. The deviations of the concentration from the mean value amount to 5—20%, depending on the discharge regime (the stability of the pinch becomes worse with increasing power). The measurements of the maximum concentration were monitored by observing the radiation scattered by the plasma at an angle 90° to the beam axis. With decreasing wavelength of the probing radiation and on going through the critical wavelength λ_c, the intensity decreases abruptly, and this serves as an independent method of checking the correctness of the measurements of the maximum concentration by means of the radiation cutoff.

The accuracy with which the maximum concentration is determined depends on the ratio Δ/a of the beam dimension to the plasma radius. As shown by model measurements on thin metallic cylinders, the distribution of the radiation in the focal plane of the lenses is close to Gaussian, and the beam dimension at the half-intensity level is $\Delta \approx (6-8)\lambda$. Measurements made on cylindrical cavities in paraffin have established that if the condition $\Delta/a < 0.5$ is satisfied the accuracy in the measurement of the maximum concentration is certain to be not worse than 10%.

The outside diameter of the plasma or its effective dimension 2a were determined at frequencies that are smaller by a factor 1.5—2 than critical for the maximum concentration. To this end, $T(\rho)$ was plotted point by point, and the effective plasma diameter was assumed to be the diameter of a metallic cylinder with a transmission curve of half-width equal to that of the experimental transmission signal of the plasma. This excludes the broadening of the transmission signal as a result of the finite width of the beam. The characteristic plasma dimension 2a measured in this case corresponds to the pinch radius at which the effective interaction of the

microwave beam with the plasma begins ($n_e(a) = 0.1n_e(0)$). This fact was verified by a study of the shape of the electron-concentration profile by the method of multiparticle probing with the aid of the plots shown in Fig. 6. For the measured profiles, if the condition $n_e(a)/n_e(0) = 0.1$ is satisfied, the refraction angle is compared with the angular aperture of the receiving system ($\theta_0 \approx 0.1$ rad) already at $\epsilon \approx .9$, so that a strong attenuation of the transmission signal sets in at $\rho \approx a$.

The point-by-point measurement of $T(\rho)$ was carried out with ρ intervals of 0.5—1 mm, depending on the width of the $T(\rho)$ signal. The amplitude of the transmission signal was read on the screen of a long-persistence oscilloscope at the point of start of the sweep. It corresponded to the instantaneous value of the transmission for a previously selected impact parameter ρ. The accuracy with which the $T(\rho)$ curve was measured was determined by the stability of the radiation source (accuracy 2—3%) and by the width of the oscilloscope beam (accuracy 3%), which is perfectly adequate, in view of the fact that the short-time instability of the plasma regimes amounts to about 10—20%.

The reflected signals were measured by an accumulation procedure and by averaging the measurements over a sufficiently large number of passages with the aid of a pulse-height analyzer. Owing to the small signal/noise ratios, measurements of the reflections were used only to monitor the maximum-concentration measurement data obtained by the cutoff method.

5. EXPERIMENTAL RESULTS

Microwave discharges in D_2, H_2, He and in mixtures of D_2 with Ar at gas pressures 1—2 atm and at microwave power inputs 4—12 kW were investigated in a number of experiments with the small plasma installation. A number of $T(\rho)$ curves averaged over many experimental points, plotted at a wavelength $\lambda = 0.55$ mm at a deuterium pressure 1.3 atm in the resonator, are shown in Fig. 9. These curves show the evolution of the transmission signals when the plasma regime is varied. With increasing power, an increase takes place in the dimension of the discharge and unblocking of the transmission signals begins.

Measurement of the maximum concentration of the plasma pinch and its characteristic dimensions at a given plasma regime were carried out by methods described in Sec. 4. The results of the measurements of the maximum concentration of the plasma are shown in Fig. 10a. The horizontal arrows denote the intervals of the powers fed to the discharge, in which, at a given wavelength, both blocked and unblocked transmission signals were observed. They can be used to plot the concentration fluctuation regions (dashed lines) for each microwave discharge regime. It is seen from Fig. 10a that the electron density on the axis deviates considerably from the mean values at large pressures and powers. It turned out that the scatter of the concentration data is due to rapid changes of the microwave power fed to the discharge. The values of the power W in Fig. 10a correspond to instantaneous-power values averaged over a time interval on the order of several minutes.

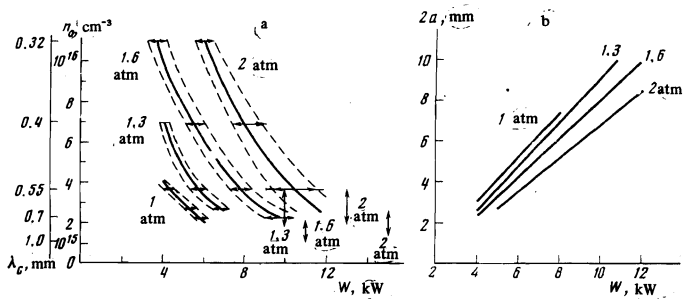

FIG. 10. a—Dependence of the maximum concentration on the discharge regime in the deuterium. b—Effective diameter of the discharge in the deuterium. Small installation.

The supplementary ordinate axis of Fig. 10a shows the wavelengths at which the probing was carried out: they correspond to the values of the critical concentration on the principal ordinate axis. The vertical arrows in Fig. 10a show the maximum concentration values as measured by reflection.

Figure 10 b shows plots of the effective diameter 2a of the plasma pinch against the power input W at different gas pressures in the resonator. It is seen from these diagrams that the diameter of the discharge increases practically linearly with the power input, and decreases with increasing gas pressure.

The radiation scattered by the plasma was observed mainly at 90° to the optical axis, but we also measured the reflection at 180° (back scattering) and at 120° using a plasma installation with an external magnetic field—the choice of the observation angle was governed by the construction of the installation. The study of the back reflection was made difficult by the presence of a strong parasitic background resulting from the reflection of the radiation by the optical elements and the walls of the microwave resonator. The results presented below of the measurement of the reflected signal pertain to observations at 90°.

By way of example, Fig. 11 shows a plot of the maximum amplitude of the reflected signal (in relative units) against the power fed to the pinch at two gas pressures in the resonator. The dashed line shows the noise level of the radiation detector. It is seen from the figure that with increasing power the reflection first increases, this being due to the transition of the discharge from the diffuse form to the pinch form and with the increase of the pinch diameter. The plasma concentration on the axis is in this case much larger than critical and the reflecting region of the plasma is quite large. Then, with increasing power, the concentration on the axis decreases and the dimensions of the transcritical region of the pinch, which reflects the radiation effectively, become smaller. The reflection signal passes through a maximum and decreases, vanishing in the detector noise. By extrapolating the experimental curves to a zero reflection signal it is possible to obtain lower bounds for the maximum pinch concentration, thereby logically supplementing the results given by the cutoff method.

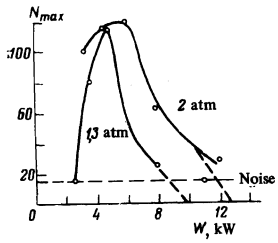

FIG. 11. Reflection from plasma, $\lambda = 0.55$ mm (N_{max} is the number of the maximal pulse-height analyzer channel corresponding to the maximum amplitude of the reflected pulse).

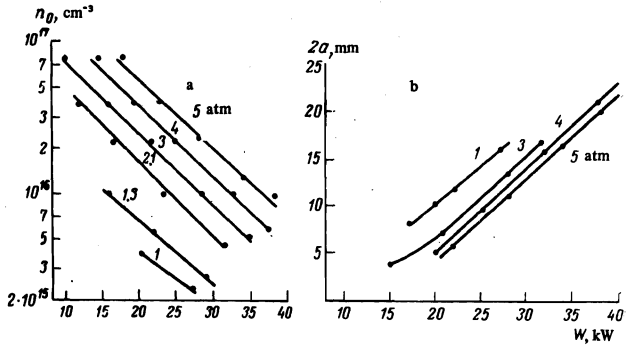

FIG. 12. a–Dependence of the maximum concentration on the discharge regimes in deuterium. b–Effective discharge diameter. Large installation.

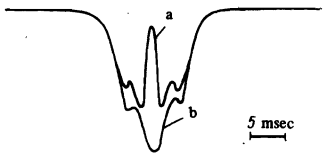

FIG. 13. Transmission signal: a–with four minima, b–with three minima. Deuterium, P = 2 atm, W = 22 kW, λ = 0.172 mm.

For a homogeneous plasma pinch, as follows from Fig. 3, a 90° reflection is possible only at $\gamma \geq 0.5$. For the remaining profiles this lower-bound estimate comes even closer to $\gamma = 1$. The vertical arrows of Fig. 10a show the intervals $(0.5-1)n_0$ for several wavelengths of the probing radiation in plasma regimes at which the 90° reflection vanishes.

Measurements of the concentration of the microwave discharge in the large installations, where the dimensions are three times larger, were carried out by the same procedure. The plasma pinch was investigated in the power-input range from 10 to 35 kW at deuterium pressures from 1 to 5 atm. In comparison with the small installation, the discharge diameter was increased by almost three times, and the maximum concentration in the indicated range of regimes varied from 10^{15} to 10^{17} cm^{-3}. Since the transverse dimensions of the microwave beam in the larger installation remain practically unchanged, the conditions for the satisfaction of the geometrical-optics approximation became more favorable, and therefore the concentration and the spatial resolutions were determined with better accuracy.

The measured maximum concentration and effective diameter of the discharge in the large installation, as functions of the pressure and of the power input, are shown in Fig. 12. It is seen from the figure that the general laws governing the variation of the concentration and the discharge dimension are the same as for the small installation.

For discharges at increased pressure and power, we observed transmission signals with four and three minima (Figs. 13a and 13b). According to the measurement on the trajectory-plotting computer, given in Sec. 3, these properties should be possessed by a pinch with a concentration jump in the near-axial region (see curve I of Fig. 7a).

To eliminate the influence of the temporal fluctuations of the plasma on the results of the measurements of the concentration profile, simultaneous probing of the pinch at four frequencies was carried out (see Sec. 2). A typical oscillogram is shown in Fig. 8. By measuring the characteristic dimension of the plasma pinch at a frequency close to critical, and by measuring the distances between minima at subcritical frequencies, it is possible to construct the experimental plot of $\gamma(\rho_{max}/a)$, from which we can select, with the aid of the curves of Fig. 6, the theoretical concentration profile that is closest to the investigated one. This procedure was used to process the oscillograms of Fig. 8. It was found that the concentration profiles are close to the function represented by plot 4 of Fig. 4.

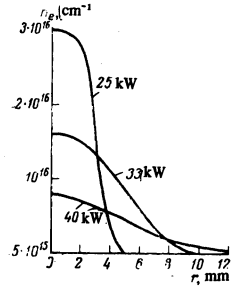

FIG. 14. Profiles of electron concentration (large installation) at different powers fed to the discharge; P = 5 atm.

By way of example, Fig. 14 shows the evolution of the concentration profiles of the pinch, obtained by the indicated method, as functions of the power supplied to the discharge at a pressure 5 atm. With increasing power from 25 to 40 kW, the density on the axis decreases from 3×10^{16} to 8×10^{15} cm^{-3}, the diameter of the discharge increases, and the electron temperature calculated from formula (3.4) of [1]

$$T_e = 7.4 \cdot 10^{21} P/n_e, \quad T_e \gg T_i,$$

increases from 1.2×10^6 to 4.6×10^6 °K.

6. CONCLUSION

The use of submillimeter generators and high-speed radiation receivers has made possible active diagnostics of a pinch microwave discharge in the wavelength range 0.1–1 mm. The maximum electron concentration of the pinch was determined by the cutoff method used for transverse probing of a radially-inhomogeneous plasma. We studied its dependence on the discharge regimes in the investigated range of concentrations ($10^{15}-10^{17}$ cm^{-3}). The results of the measurements by the cutoff method are monitored by observing the radiation reflected from the plasma. The four-frequency probing procedure makes it possible to measure, with one passage of the pinch through the microwave beams, not only the maximum concentration on the axis and the characteristic dimensions of the plasma, but also to determine the electron-concentration distribution function averaged over the width of the microwave beam. Measurements of the concentration profile by a refraction procedure on a large installation are more accurate, owing to the increase of the transverse dimensions of the pinch. This installation also revealed concentration-profile irregularities corresponding to a jump of the density in the region next to the axis. The high speed of the procedure makes it possible to observe temporal pulsations of the internal structure of the pinch.

Observation of concentration profiles with a density jump in the near-axis region of the discharge conforms to the hypothesis that a double electron layer exists between the hot core and its surrounding shell, while the values of the electron density on the pinch axis yields for the electron temperature of the nucleus a value on the order of 10^6 °K.

[1] P. L. Kapitza, Zh. Eksp. Teor. Fiz. **57**, 1801 (1969) [Sov. Phys.-JETP **30**, 973 (1970)].
[2] P. L. Kapitza and S. I. Filimonov, Zh. Eksp. Teor. Fiz. **61**, 1016 (1971) [Sov. Phys.-JETP **34**, 542 (1972)].
[3] P. L. Kapitza, Zh. Eksp. Teor. Fiz. **58**, 377 (1970) [Sov. Phys.-JETP **31**, 199 (1970)].
[4] M. B. Golant, R. L. Vilenskaya, E. A. Zyulina, Z. F. Kaplun, A. A. Negirev, V. A. Parilov, T. B. Rebrova, V. S. Savel'ev, Prib. Tekh. Eksp. No. 4, 136 (1965).
[5] E. A. Tishchenko, Prib. Tekh. Eksp. No. 5, 215 (1970).
[6] K. A. Zhdanov, V. G. Zatsepin, and E. A. Tishchenko, Prib. Tekh. Eksp. No. 1, 138 (1974).
[7] E. A. Tishchenko, V. G. Zatsepin, and K. A. Zhdanov, Prib. Tekh. Eksp. No. 1, 153 (1974).
[8] M. Born and E. Wolf, Principles of Optics, Pergamon, 1970 (Russ. transl., Nauka, 1973, p. 128).
[9] G. P. Prudkovskiĭ, in: Elektronika bol'shikh moshchnostei (High-Power Electronics), Vol. 3, Nauka, 1961, p. 70.

Translated by J. G. Adashko
62